This article was downloaded by: [University of Genova], [serena cattari]
On: 02 April 2013, At: 23:58
Publisher: Taylor & Francis
Informa Ltd Registered in England and Wales Registered Number: 1072954 Registered office: Mortimer House, 37-41 Mortimer Street, London W1T 3JH, UK

International Journal of Architectural Heritage: Conservation, Analysis, and Restoration
Publication details, including instructions for authors and subscription information:
http://www.tandfonline.com/loi/uarc20

# Modernist URM buildings of Barcelona. Seismic vulnerability and risk assessment

R. Gonzalez-Drigo [a], J.A. Avila-Haro [a], A.H. Barbat [a], L.G. Pujades [b], Y.F. Vargas [b], S. Lagomarsino [c] & S. Cattari [c]

[a] Department of Structural Engineering, Polytechnic University of Catalunya. UPC-Barcelona-TECH, Barcelona, Spain

[b] Department of Geotechnical Engineering and Geo-Science, Polytechnic University of Catalunya. UPC-Barcelona-TECH, Barcelona, Spain

[c] Department of Structural and Geotechnical Engineering, University of Genoa, Genova, Italy

Accepted author version posted online: 18 Mar 2013.

To cite this article: R. Gonzalez-Drigo , J.A. Avila-Haro , A.H. Barbat , L.G. Pujades , Y.F. Vargas , S. Lagomarsino & S. Cattari (2013): Modernist URM buildings of Barcelona. Seismic vulnerability and risk assessment, International Journal of Architectural Heritage: Conservation, Analysis, and Restoration, DOI:10.1080/15583058.2013.766779

To link to this article: http://dx.doi.org/10.1080/15583058.2013.766779

Disclaimer: This is a version of an unedited manuscript that has been accepted for publication. As a service to authors and researchers we are providing this version of the accepted manuscript (AM). Copyediting, typesetting, and review of the resulting proof will be undertaken on this manuscript before final publication of the Version of Record (VoR). During production and pre-press, errors may be discovered which could affect the content, and all legal disclaimers that apply to the journal relate to this version also.

PLEASE SCROLL DOWN FOR ARTICLE

Full terms and conditions of use: http://www.tandfonline.com/page/terms-and-conditions

This article may be used for research, teaching, and private study purposes. Any substantial or systematic reproduction, redistribution, reselling, loan, sub-licensing, systematic supply, or distribution in any form to anyone is expressly forbidden.

The publisher does not give any warranty express or implied or make any representation that the contents will be complete or accurate or up to date. The accuracy of any instructions, formulae, and drug doses should be independently verified with primary sources. The publisher shall not be liable for any loss, actions, claims, proceedings, demand, or costs or damages whatsoever or howsoever caused arising directly or indirectly in connection with or arising out of the use of this material.

ACCEPTED MANUSCRIPT

# Modernist URM buildings of Barcelona. Seismic vulnerability and risk assessment.

Gonzalez-Drigo R. [a], Avila-Haro J.A. [a], Barbat A.H. [a], Pujades L.G. [b], Vargas Y.F. [b] Lagomarsino S. [c] and Cattari S. [c]

[a] Department of Structural Engineering. Polytechnic University of Catalunya. UPC-Barcelona-TECH. Barcelona. Spain.

[b] Department of Geotechnical Engineering and Geo-Science. Polytechnic University of Catalunya. UPC-Barcelona-TECH. Barcelona. Spain.

[c] Department of Structural and Geotechnical Engineering. University of Genoa. Genova, Italy.

Ramon González-Drigo.

Department of Structural Engineering. Polytechnic University of Catalunya.

C/Urgel 187, 08036 Barcelona, Spain.

Email: jose.ramon.gonzalez@upc.edu

Downloaded by [University of Genova], [serena cattari] at 23:58 02 April 2013

# Modernist URM buildings of Barcelona. Seismic vulnerability and risk assessment.

The main objective of this work is to assess the vulnerability and seismic risk of typical existing URM modernist buildings and aggregates situated in the Eixample district of Barcelona, part of the architectural heritage of the city. The context of the analysis is the methodology proposed by the Risk-UE project. The buildings are characterized by their capacity spectrum and the earthquake demand is defined by the 5% damped elastic response spectrum, considering deterministic and probabilistic earthquake scenarios. A discussion is made regarding the basis of the seismic damage states probabilities and the calculated damage index. An important research effort has been focused on the buildings modelling. All the architectural elements and their mechanical properties have been studied and evaluated accurately. It has been evidenced that a

ACCEPTED MANUSCRIPT

ACCEPTED MANUSCRIPT

detailed and complete knowledge of all the structural elements existing in this type of buildings influence directly their behavior and hence the calculations and the results. The analysis of the isolated buildings and of the aggregate building has been performed for both mentioned seismic scenarios. Finally, a complete discussion of the results is included.

Keywords: Unreinforced masonry, modernist architecture, capacity spectrum method, vulnerability, fragility, risk assessment.

Downloaded by [University of Genova], [serena cattari] at 23:58 02 April 2013

# 1 Introduction

In the Mediterranean area, modern cities accumulate a large number of buildings, infrastructures and facilities that result in an important concentration of socioeconomic value and in high population density. (EUROSTAT, 2011; US Bureau-of-the-Census, 1991). At present the 75% of European people live in cities with more than 100.000 inhabitants.

The seismic hazard is not negligible in this area (Jiménez, et al., 2001; Grünthal, et al., 1999; Egozcue, et al., 1991) and the seismic risk is higher than expected due to the high vulnerability of constructions built in the urban centers where a significant number of the current buildings are constructed with unreinforced brick masonry and without any consideration of the seismic actions. Most of these buildings are more than 100 years old, which means that they largely overpass the service life initially supposed for them. In addition, several circumstances, as the material degradation, some aggressive retrofitting and refurbishing works, and the changes in the building load conditions, increased their overall vulnerability (Figure 1). Therefore, the

ACCEPTED MANUSCRIPT

ACCEPTED MANUSCRIPT

vulnerability of these URM buildings, the important population density and the not negligible seismic hazard in the region, decisively increased the seismic risk in these urban areas.

Recent studies in earthquake engineering are oriented to the development, validation and application of techniques to assess the seismic vulnerability of existing buildings. (Yépez, et al., 1996; Barbat, et al., 1998; Barbat, et al., 2006a; Barbat, et al., 2006b ; Carreño, et al., 2007; Barbat, et al., 2008; Lantada, et al., 2009; Pujades, et al., 2012)

Barcelona is a city located in a low-to-moderate seismicity region in the northeast of the Iberian Peninsula and in the western coast of the Mediterranean Sea. During the 19th century, a high population pressure and a city oppressed by the medieval walls were the determinant circumstances that generated a major urban expansion project. During the first period of this expansion, from 1860 to 1940, most of the buildings constructed were unreinforced masonry (URM) buildings. Today, many of those buildings, more than one hundred years old, still stand (Lantada, 2007) and are part of the architectural heritage of Barcelona. The main objective of this work is to assess the seismic vulnerability and risk of those buildings, situated in the Eixample district of Barcelona by using the method proposed in the Risk-UE project (Milutinovic & Trendafiloski, 2003). The structural analysis is performed by means of the TreMuri computer program (Lagomarsino et al. 2008) that has been specifically developed for the linear and nonlinear analysis of URM buildings. Different MATLAB codes (Matlab v.2009b, The MathWorks) have been developed in order to obtain the fragility curves and the damage index corresponding to each studied model. The most important results of this article are the fragility curves and the damage probability matrices obtained for this building typology.

Downloaded by [University of Genova], [serena cattari] at 23:58 02 April 2013

ACCEPTED MANUSCRIPT

ACCEPTED MANUSCRIPT

## 2 The urban expansion project and the buildings

In 1850, Barcelona still remained as a walled city; in 1854 the decree for the urban expansion project was approved. The urban planning was designed in 1859 by the civil engineer Ildefons Cerdá. Thus, the mediaeval walls were demolished and the plain area between the city walls, the Mediterranean coast and the Collserola Hills was opened to be urbanized (Lantada, 2007). The new district was called Eixample (enlargement). Figure 2 shows a typical section of the Eixample district.

Nowadays, the Eixample district has 247.418 inhabitants, a population density of 33.148 inhabitants/km2 and 8.658 buildings. Most of these buildings were built before 1960, being 1931 the average year of construction. Today, the unreinforced brick masonry buildings suppose nearly 70% of the buildings of the Eixample (Lantada, 2007).

Although the buildings were built independently, most of them were constructed by sharing the lateral load walls with the existing adjacent buildings. In consequence, the masonry buildings of the Eixample district form large squared aggregates constituting the so called islands or blocks, following the urban framework shown in Figure 2. The framework of the urban plan is a net of squared blocks sided 133m long on average. The streets, 25 m wide on average, cross orthogonally between the blocks. This framework makes buildings design conditional to the orthogonal shape of the blocks and the buildings can be fitted together if they are outlined following repetitive patterns. In the mid side of the blocks, central buildings have orthogonal perimeters with a ratio between the dimensions in plan of at least 2 to 1. At the end of the blocks, the corner buildings are more irregular and have a typical pentagonal perimeter. Figure 3 shows

ACCEPTED MANUSCRIPT



Downloaded by [University of Genova], [serena cattari] at 23:58 02 April 2013

ACCEPTED MANUSCRIPT

the floor plan of an actual and characteristic row of aggregate buildings, which includes the buildings analyzed in this study. In this figure, the names of the buildings studied in this article are also shown. In any case, even considering modern buildings, the shape in plane of the buildings does not depend on the building typology (unreinforced masonry or reinforced concrete), but it only depends on the geometrical fit of the building into the block aggregate.

Downloaded by [University of Genova], [serena cattari] at 23:58 02 April 2013

### *2.1 The buildings*

In this work we evaluated 3 existing isolated buildings and an aggregate of 2 buildings. All of them have 7 stories. The buildings correspond to a row aggregate of a block in a main street in the city of Barcelona. Figure 4 shows the façades of these buildings, which are very representative for the Eixample district; all of them are URM structures with load-bearing walls. Foundations are shallow, running through surface pads under the walls or, in case of more recent buildings, they are isolated foots under concrete pillars.

We will refer to the rectangular buildings as M01, M02 and M03 (Figure 3). The aggregate corresponds to the sequence M01-M01. This means that the aggregate has been designed by means of two twin URM buildings built together. We will refer to this aggregate as A01. Figure 3 shows the existing aggregate. Other data relative to storey heights, walls density, loads and walls thicknesses are shown in Table 1, Table 2, Table 3 and Table 4.

The resistant elements are bearing walls and, in the ground floors, there may also exist masonry columns or cast iron columns. In general, these buildings only have the necessary elements to

ACCEPTED MANUSCRIPT

ACCEPTED MANUSCRIPT

ensure the stability of the structure. More details of the specific architectonic features of the masonry buildings of the Eixample district are given by Paricio (2008),

### *2.2 The walls*

The walls of the street façade, the inner courtyard of the block and the walls between buildings, usually called intermediate walls, are the main bearing walls. In the first story, metallic columns (foundry columns in some buildings) and girders are present (Figure 5) and, usually, above those girders and for all the upper stories, additional bearing walls (usually two) are added parallel to the façades. This constructive solution, which avoids placing inner walls for the first or for the first two stories, is very common, permitting larger clear spaces, allowing the ground floors being used for trading or catering activities and for office or administrative activities in the mezzanines. In addition, each building has one or more nuclei around the staircases and small internal courtyards made to provide natural light to the internal rooms. These nuclei are partially closed by masonry walls and are also used as bearing elements (Figure 6b). Finally these buildings also have a secondary system of interior walls which, in general, do not have a significant contribution to their strength; these walls have a thickness lower than 10 cm and their main function is to separate the volumes and to provide acoustic insulation.

In general, the inner walls, which can reach lengths of up to 10 m, are poorly connected or connected neither to the façades nor to the walls between adjacent buildings and, therefore, they cannot behave as bracing walls. Furthermore, when there are openings for doors, windows or balconies, they have lintels or parapets of variable dimensions; the wall sections over lintels or

Downloaded by [University of Genova], [serena cattari] at 23:58 02 April 2013

ACCEPTED MANUSCRIPT

ACCEPTED MANUSCRIPT

parapets are extremely weak areas where cracks due to the effect of differential movements can be observed.

Both the street façade and the inner courtyard walls have significant openings with windows and balconies. As the level increases, these openings are smaller, so the presence of large openings is usual in the first levels, making these walls weaker even if their thickness is greater. Figure 6 shows a complete graphical description of one of the studied buildings (M01 in Figure 3). The intermediate walls shared between adjacent buildings are solid and do not present any opening. The first building raised up incorporates an intermediate wall with a thickness of 30 cm at the first floor. From the second level until the top of the building, the thickness of this wall diminishes to 15 cm. Over the entire height of the wall, some unreinforced masonry columns are embedded at a regular distance of 3.5 m to 5 m from each other. When the adjacent building is raised, it directly shares the intermediate wall of the first story and it complements until 30cm the thickness of the wall at the upper floors. This means that in each building the maximum support of the floor beams is 15 cm on these walls (see Figure 7). Details of the organization of these walls are shown in Figure 8.

An interesting geometric parameter is the density of walls which is defined as the ratio of the area of the cross section of all the walls of a specific story to the total area of the floor (Gonzáles, 2010). For the analyzed buildings, Table 1, Table 2, Table 3 and Table 4 include the density of walls, the values of thickness corresponding to the different walls and the dead and live loads corresponding to different levels. For all the buildings, we took into account only the walls having a thickness greater than 10 cm. All the values are given for different stories.

Downloaded by [University of Genova], [serena cattari] at 23:58 02 April 2013

ACCEPTED MANUSCRIPT

ACCEPTED MANUSCRIPT

*2.3 The floors*

From 1860 to 1960, most of the floors of the unreinforced buildings of the Eixample were solved with unidirectional slabs. But, at different periods, the materials of the elements used for the floors changed. From 1860 to 1890 approximately, the floors were one-way timber floors with single or overlapped wood planks including an additional concrete topping. From 1890 to 1940, iron beams and brick vaults were widely used. This is the case of the studied buildings (Figure 9 and Figure 10). After 1940, during the Spanish postwar period, there was a time of shortages when iron and steel were scarce. Therefore, the use of reinforced concrete beams and brick vaults or ceramic blocks was the solution for the floors.

The buildings studied in this article as typical for the URM building of the Eixample, were built between 1920 and 1935. Basically, their floors are composed of girder beams whose heads lay on bearing walls or on main beams. There are main beams only at the first level floor, sustained on cast iron columns (Figure 5 and Figure 6b), allowing large open spaces as described before. The support length of the girder beams on the perimeter walls depends on the wall thickness. For intermediate walls, the supporting length is 15 cm. In the case of façade walls, it is 30 cm for lower stories and 10-15cm for upper stories. This very common solution for the floors required girder beams with a separation ranging from 60 to 120 cm. The floor thickness is reduced, varying from 15 up to 20 cm, while the timber floors, older than these, have thicknesses that duplicate and even triplicate these values. Between the girder beams, the floor is solved by placing small vaults or, in more recent cases, case-bays. In all the cases, those elements spring on the girders flanges. In addition, the groins are filled with plaster and chippings and, then, the

Downloaded by [University of Genova], [serena cattari] at 23:58 02 April 2013

ACCEPTED MANUSCRIPT

ACCEPTED MANUSCRIPT

floor is smoothed, leveled and covered with the pavement (Figure 9 and Figure 10). Due to their stiffness, the single bridging is not needed in these floors.

The total weight is due to the dead loads and the live loads. The load values used in this article are in accordance to the characteristic values from the city council regulations documents (Paricio, 2008) previous to all the building codes that appeared and were currently in force after 1960 (Ministerio de la Vivienda, 1963; Ministerio de Fomento, 1988; Ministerio de la Vivienda, 2006). In our structural analyses, we assigned 200 kg/m2 to the floor weight; the load due to the distribution walls has been estimated in 100 kg/m2; the weight of an ordinary tiled floor pavement has been evaluated in 50 kg/m2 and has to be added to the corresponding floor permanent load. In consequence, a permanent load of 350 kg/m2 and a variable load of 200 kg/m2 are the considered values in the calculations of the intermediate floors, while 350 kg/m2 and 100 kg/m2 are those considered for the terrace roofs.

Downloaded by [University of Genova], [serena cattari] at 23:58 02 April 2013

### *2.4 The bricks and the mortars*

The brickwork of the analyzed buildings uses solid prismatic bricks, made of fired clayey soils. These bricks are easy to handle and their thickness is lower than 12 cm. Ordinary bricks (29x14x5,5cm) were mainly used in bearing walls; bricks of 4,5 (29x14x4,5cm) were used in division walls; medium brick (29x14x3cm) and thin bricks (29x14x2cm) were used in the construction of vaults. According to the firing grade, there were four categories of bricks. As the firing grade increases, the strength and the apparent density of bricks and brickwork increase (Schindler & Bassegoda, 1955). It was a common practice to select the most resistant bricks for

ACCEPTED MANUSCRIPT

ACCEPTED MANUSCRIPT

very loaded walls. As the commercialization of ceramic hollow bricks started later, in 1940, they were not used in the analyzed buildings.

The studied buildings were built in the late 19th and early 20th centuries and most of their bricks were manufactured in continuous kilns; therefore they have similar properties. In general, they show a rough texture that favours a good adherence to the support. Their surface is rather compact without observable gaps like hollows and holes. Breakage of bricks shows a fine and regular grain and very few impurities of appreciable size in the matrix. There are not vitrified zones. The colour varies between red for the bricks with lower strength (7MPa) and a more or less pale ochre for the higher strength ones (15MPa).

The strength demand conditioned the mortar selection for the brickwork. In order of decreasing strength, the mortars used were: Portland mortars, natural mortars (roman cement), lime mortars and bastard mortars.

### *2.5 The brickwork and the walls organization*

In the buildings studied in this article, the different brickwork differs according to the wall function and its corresponding thickness (P.I.E.T. 70, 1971). The thickness of most of the partition walls was lower than 6,5 cm, without including the plastering. These walls are made of medium and thin solid bricks. In some cases, double partition walls are used, with a thickness between 6,5 and 9 cm without including the plastering. For all the bearing walls, the brickwork is made using solid bricks. Thus, the corresponding thickness is a multiple of the brick width (15 cm). Without taking account of plastering, the usual thicknesses are: 15cm, 30 cm, 45cm, 60 cm

Downloaded by [University of Genova], [serena cattari] at 23:58 02 April 2013

ACCEPTED MANUSCRIPT

ACCEPTED MANUSCRIPT

and 75 cm. The brickwork with ordinary brick in buried walls and in stairway cases is made with hydraulic lime mortar or with Portland mortar. The exterior brickwork is made with lime mortar. For medium range loads, the brickwork uses bastard mortar and, for main loads or in slender pillars, resistant bricks and Portland cement mortar are used.

Table 5 shows the values of the design strength of the brickwork made with solid bricks and different mortars. It should be considered that all the values are design values and that they have been obtained by reducing the corresponding characteristic values of strength with a coefficient of 2,5.

### *2.7 Openings and lintels*

In the URM buildings of the Eixample, the doorways and window spans use discharging arches or iron lintels (Figure 11). For openings in thin walls, as is the case of the distribution walls, the option was to use wood elements for the lintels of the doorways and windows. In big openings, the lintels are made with two, three or more beams, according to the wall thickness (one beam for each 15 cm of wall thickness), and are placed parallel to each other. The beams are fastened with bolts housed into iron tubes that maintain the beams at the required distance. The length of the beams support onto the walls can be taken as the edge length of the beam but, in any case, it is inferior to 20 cm (Figure 12).

## 3 The structural analysis

TreMuri is a widely recognized and widespread computer program for the analysis of masonry structures. It was developed at the University of Genoa (Lagomarsino, et al., 2008) in order to

ACCEPTED MANUSCRIPT



Downloaded by [University of Genova], [serena cattari] at 23:58 02 April 2013

ACCEPTED MANUSCRIPT

simulate the non linear behavior of masonry structures. Its advanced, innovative computational model uses macroelements and constitutive laws based on experimental tests (Galasco, et al., 2006, Calderini, et al., 2009). For the analysis of masonry structures, this program, by means of the effective macroelement approach, adopts an accurate modeling strategy but without heavy computational load. The macroelement shear model (Gambarotta & Lagomarsino, 1997) is a macroscopic representation of a continuous model in which the parameters are directly related to the mechanical properties of the masonry elements. Complete 3D models of URM structures can be obtained by assembling 2-nodes macroelements, representing the non-linear behavior of masonry panels and piers. This modeling strategy has been implemented in the TreMuri program with non-linear static and dynamic analysis procedures. By means of internal variables, the macroelement takes into account both the shear-sliding damage failure mode and its evolution, controlling the strength and stiffness degradation and rocking mechanisms with toe crushing effect. URM building models can be obtained by assembling plane structures, walls and floors.

The program allows performing non-linear static and dynamic analyses of masonry structures using a well defined seismic action. These characteristics distinguish TreMuri from other computer programs which mostly focus on reinforced concrete and steel structures.

The buildings studied in this article are made of solid clay ceramic bricks. They have regular floors in plan and a homogeneous distribution of the openings of the walls, excepting the first floor. These features assure their adequate modelling by using macroelements of the TreMuri computer program.

Downloaded by [University of Genova], [serena cattari] at 23:58 02 April 2013

ACCEPTED MANUSCRIPT

ACCEPTED MANUSCRIPT

The buildings analyzed in this study were modeled on the basis of original floor plans and architectural drawings as well as other useful documents which supplied a selection of profitable technical data. Several manuals and books were used (Schindler & Bassegoda, 1955). Other data were completed with existing laboratory tests results or have been obtained on the basis of technical reports of restoration of URM buildings of Barcelona and based on the guidelines and judgment of architects and civil engineers. The analyses are performed in order to obtain the seismic behavior of isolated buildings as well as of aggregated buildings.

The mechanical properties used in this study have been obtained on the basis of recent technical reports, results of existing mechanical tests results and values included in documents that are contemporary with the analyzed buildings. The guidelines and judgment of architects and civil engineers with expertise on these types of materials and constructions have also been taken into account. The main properties of the masonry walls and columns are: average specific weight, $\rho$=18 kN/m$^3$, average elastic modulus E=2650 MPa, average shear modulus, G=589 MPa, average shear strength $\tau$=7,95x10$^{-2}$ MPa, average compression strength $\sigma$=2,65 MPa. Moreover, concerning the floors, an average total load (dead loads G + live loads Q) of 4,5 kN/m$^2$ for the last level, and 5,5 kN/m$^2$ for the rest of the levels.

The modal analysis (Table 6) was performed for each building and the aggregate using the TreMuri software. From these analyses we can observe that the first and second modes of vibration are translational for the four structures, and that the third mode of each model is rotational.

## 4. The earthquake scenarios

ACCEPTED MANUSCRIPT



Downloaded by [University of Genova], [serena cattari] at 23:58 02 April 2013

ACCEPTED MANUSCRIPT

The seismic hazard can be evaluated using deterministic and probabilistic methods. The deterministic method assumes that the historical seismicity contains sufficient information to assess the seismic hazard of a certain region. On the other hand, the probabilistic approach evaluates the seismic hazard by linking a probability of occurrence to the tectonic and seismicity information of a specific region. For the City of Barcelona, the deterministic scenario was defined by the 1448 Cardedeu earthquake, which occurred at an epicentral distance of 25 km with a 7 km depth and an epicentral intensity of VIII (EMS'98) (Secanell, et al., 2004). The probabilistic scenario was obtained based on the attenuation law of Ambrasseys et al. (1996) and on the regional parameters obtained by Secanell et al. (2004) with the software CRISIS-99.

For both scenarios, Irizarry (2004) fitted the analytical formulations proposed in Eurocode 8 and RISK-UE project (Milutinovic & Trendafiloski, 2003), by varying the acceleration response spectra obtained for four different soil zones of Barcelona defined in previous studies by Cid (1998). The reliability of both approaches was evaluated by calculating the Root Mean Square and error percentage between each approach and the target spectrum obtained from the seismic hazard analysis. The RISK-UE approach was selected for the calculation of the 5 percent-damped demand spectra.

The seismic microzonation of the soils of Barcelona considers four seismic zones with different soil types; namely A, I, II and III (Cid 1998, Irizarry 2004). Soils in zone A correspond to rocky outcrops, soils in zone I correspond to very soft soils, typical of deltaic zones; in zone II, soils are intermediate soft soils and in zone III, soils are intermediate hard. Since the Eixample district is located mostly in zone II, this type of soils has been selected for the assessment of the

ACCEPTED MANUSCRIPT



Downloaded by [University of Genova], [serena cattari] at 23:58 02 April 2013

ACCEPTED MANUSCRIPT

expected damage. Figure 13 shows the 5% damped elastic response spectra corresponding to the deterministic and probabilistic earthquake scenarios.

## 5. The buildings damage states

The Eixample district where the analyzed buildings are located is placed in the soil zone II. The analyses performed to obtain the seismic behavior of these structures were made by using the response spectrum of this zone.

The procedure followed for the capacity and fragility assessment is based on the capacity spectrum method, which provides a graphical representation of the capacity curve of the structure and compares it to the seismic demand spectra (ATC-40, 1996).

According to the guidelines described in ATC-40, the capacity curves for each analyzed building are obtained by means of a pushover analysis. The capacity curves obtained in terms of base shear and roof displacement are converted to the Acceleration-Displacement Response Spectra (ADRS) format (ATC-40, 1996). Figure 14 shows the capacity curves and the capacity spectra for the building A01 in the +X and +Y directions. Figure 15 and figure 16 show the capacity curves in ADRS format and for the +X and +Y directions, respectively, for the isolated building M01 and for the aggregate A01. Additionally, the demand spectra for the deterministic and probabilistic seismic scenarios are also included in ADRS format.

The response spectrum is converted from the standard Sa-T format to the ADRS format (ATC-40, 1996). The next step of the analysis consists in developing fragility curves for each building

Downloaded by [University of Genova], [serena cattari] at 23:58 02 April 2013

ACCEPTED MANUSCRIPT

ACCEPTED MANUSCRIPT

model. This part of the analysis is performed according to the simplified procedure proposed in the RISK-UE project (Milutinovic & Trendafiloski, 2003).

The assessment of the buildings damage requires the definition of different damage states in order to predict several types of losses due to structural damage. The number of damage states and the way used to define them vary from one guideline to another. For example, the methodologies exposed in HAZUS'99 (FEMA/NIBS, 1999) and RISK-UE (Faccioli & Cauzzi, 2006) define four damage states: Slight ($ds_1$), Moderate ($ds_2$), Severe ($ds_3$) and Complete ($ds_4$). The RISK-UE methodology was applied in this work, in which the damage states depend on the parameters of the bilinear representation of the capacity spectrum ([$Sd_y$, $Sa_y$] and [$Sd_u$, $Sa_u$]) (Lagomarsino, et al., 2002).

## 6. Fragility curves and damage indices

The probability of reaching or exceeding a given state of damage is represented by fragility curves. There are several available methods to develop fragility curves, albeit their refinement and quality depend on the field of application and their use. These methods can be classified in four main types: judgment-based (expert opinions), observational/empirical (experiments), analytical (models), and hybrid (two or more of the other methods). In the selection of one or another method, it is mandatory to take into account the available information, the level of knowledge of the failure modes, and the disposable resources. These curves are described by lognormal cumulative probability functions. Their main purpose focuses on expressing the degree of damage that a structure or a set of structures will experience when exposed to ground motion actions.

ACCEPTED MANUSCRIPT



Downloaded by [University of Genova], [serena cattari] at 23:58 02 April 2013

ACCEPTED MANUSCRIPT

The need to express the degree of damage in terms of probability is due to the variation in response of the studied structures because of the large number of uncertainties related to aspects such as the action to which they are subjected, the use of generic information instead of specific data, the soil where they are located, as well as those uncertainties inherent to the structure and its modeling (material properties, structural type, use, regularity, symmetry, etc.).

Downloaded by [University of Genova], [serena cattari] at 23:58 02 April 2013

The assumption of using lognormal distributions can be justified as prudent because of its adequacy for representing the statistical variation of many material properties and seismic response variables (Keneddy, et al., 1980). For the purposes of this work, the spectral displacement will be used as the parameter that defines the seismic action. The probability of reaching or exceeding a defined damage state, $ds_i$, due to a spectral displacement, sd, is (FEMA/NIBS, 1999)

$$P[ds \geq ds_i | sd] = \Phi\left[\frac{\ln\left(\frac{sd}{sd_{ds_i}}\right)}{\beta_{ds_i}}\right] \quad (1)$$

where $\beta_{dsi}$ is the standard deviation of the natural logarithm of the spectral displacement at which the structure reaches the damage state $ds_i$, $sd_{dsi}$ , is the mean value of this spectral displacement, and $\Phi$ is the normal standard cumulative function.

For each damage state, the mean value of the corresponding fragility curve is obtained from the capacity spectrum using simplifying assumptions. Then, for obtaining the standard deviations, it

ACCEPTED MANUSCRIPT

ACCEPTED MANUSCRIPT

is assumed that the probability of reaching or exceeding that particular damage state and this spectral displacement is 50% and that the seismic damage of the buildings follows a binomial probability distribution (see Table 7) or an equivalent Beta distribution. A detailed explanation on how the fragility curves are obtained from the capacity spectra can be found in (Lantada, et al., 2009). Figure 17 shows the fragility curves for the A01 building in the +X and +Y directions. Table 8 shows the mean values and the standard deviations of the fragility curves corresponding to the analyzed buildings and aggregate.

The procedure used to model and, subsequently, to evaluate the capacity of the buildings, determines the damage index usable to quantify the damage accumulated by the structure. In our case, the buildings are modeled using macro-elements, and their capacity is evaluated on the basis of an equivalent SDOF system. Therefore, using these models and procedures to calculate their capacity, only global response quantities and rough estimations of the global damage can be calculated (Kappos, 1997).

The damage index, DI, also known as the mean damage value (normalized), works as an indicator of the global expected damage in the structure. It is also used to generate seismic risk scenarios in urban areas. The main characteristic of this value is the ease and prompt evaluation of the seismic behavior of the structures. It is defined as:

$$DI = \frac{1}{n} d_m = \frac{1}{n} \sum_{i=0}^{n} i \times P(ds_i) \qquad (2)$$

ACCEPTED MANUSCRIPT



Downloaded by [University of Genova], [serena cattari] at 23:58 02 April 2013

ACCEPTED MANUSCRIPT

where DI is the damage index, n is the number of damage states, and $P(ds_i)$ is the probability that a damage state i occurs. According to this definition, this damage index is a quantity in the range [0, 1], so that the value 0 is associated to the absence of damage in the structure, while the value of 1 (100%) is associated to collapse, understood as a full or complete damage.

Table 9 and Table 10 show the main results of this work. Table 9 corresponds to the deterministic earthquake scenario. Table 10 corresponds to the probabilistic case. These results are discussed in the following section.

Downloaded by [University of Genova], [serena cattari] at 23:58 02 April 2013

**7. Discussion of the results**

The main objectives of this work have been to study URM modernist buildings typical of the Eixample district of Barcelona and to assess their seismic vulnerability and risk. The evaluation has been made with the advanced methods proposed in the Risk-UE project. A discussion is made on the basis of the damage states probabilities and the damage index obtained for different isolated buildings and for the aggregate. We analyzed the buildings in two directions: +X (parallel to the street) and +Y. Both directions correspond to the main inertia directions of the buildings. +X is the direction corresponding to the shorter side of the buildings and is also the direction where the buildings are aggregated, while +Y is orthogonal to +X, and corresponds to the longest side of most of the buildings.

An important effort has been focused on the buildings modeling. It has been evidenced that all the existing structural elements of the analyzed buildings influence directly their behavior and, hence, on the calculations and results. In our study, existing floor plans of the analyzed buildings

ACCEPTED MANUSCRIPT

ACCEPTED MANUSCRIPT

did not include all structural details. This was usual at the beginning of the 20th century when most architects used to include in their projects only partial information. To complete these undocumented building details, a methodic research of contemporary bibliographic funds and public architectural databases was performed. The research included also several field works that allowed checking the buildings and their structural elements today. This research allowed evolving the building models from their initial conception, incomplete in any case, to the current one, which we consider accurate and reliable. Several conclusions have been outlined from the analysis performed by using these models.

Within the earthquake scenarios context, and according to the obtained fragility curves (Figure 17), the probabilistic scenario shows higher damage values and worst performance than the deterministic scenario, in consistency with the values of the PGA obtained for both scenarios. This pattern is common for both analyzed directions. Figure 18 displays the data of Table 9 and Table 10 summarizing these trends. Associated to the deterministic scenario, we obtained higher values of the damage index related to the +X direction than to the +Y direction. This difference is negligible only in the case of the building M03 which has a more squared floor plan than the other analyzed buildings. Except building M03, the damage state probabilities in the +X direction are centered between the slight and moderate states, while for the +Y direction the damage is centered between the no damage and the slight damage states (Figure 18). These results indicate that the expected damage associated to these URM buildings of Barcelona is predominantly moderate with non negligible values of exceedance probability related to the severe damage state (Figure 18, Table 9 and Table 10).

Downloaded by [University of Genova], [serena cattari] at 23:58 02 April 2013

ACCEPTED MANUSCRIPT

ACCEPTED MANUSCRIPT

An interesting observation can be made comparing the results related to the isolated building M01 to the results obtained for the aggregate A01, which is, in fact, the building M01 replicated. The damage indices results for the isolated building and for both analyzed directions (+X and +Y) are higher than those obtained for the aggregate. This difference is remarkable especially when we evaluate the difference related to the +Y direction where the damage index of the isolated building is 0,234 while the corresponding to the aggregate is 0,191. The same trend is obtained when the damage indices are calculated for deterministic and probabilistic scenarios. The differences related to both analyzed directions indicate that the seismic performance is improved when the buildings are aggregated. Probably, also in this case, because the aggregate is more regular than the isolated building, particularly in the +Y direction.

In all the cases, and for both scenarios, the analysis of the fragility curves and damage indices indicates that the buildings have a better performance in the +Y direction . Regarding the wall density, and in an attempt to relate the seismic performance in each direction with the wall density, an additional analysis has been performed. For the upper levels (levels from 2 to 7), the +X direction the buildings have thicker walls than in the +Y direction, but also a larger number of openings which are not present in the +Y direction. In spite of the presence of openings, the wall density in +X direction remains slightly higher than the one in +Y direction (see the Tables 1 to 4). For the first level, the wall density in the +Y direction is significantly higher than in the +X direction. This is due to the absence of inner walls at this level. The presence of metallic columns and girders allows an open space at this level which is commonly used for trading or catering activities. Nevertheless, the relationship between damage and wall density is somehow unclear since, for upper stories, the wall density is slightly higher in the +X direction, while the

Downloaded by [University of Genova], [serena cattari] at 23:58 02 April 2013

ACCEPTED MANUSCRIPT

ACCEPTED MANUSCRIPT

seismic performance related to the +X direction is worse. In our opinion, rather than considering parameters related to the area of the cross section of the walls, mechanical parameters related to the inertia of the walls in each direction should be evaluated and correlated in order to explain the greater vulnerability in the +X direction.

The initial stiffness of the buildings in both directions was evaluated (Table 11). The results indicate a greater stiffness associated to the +Y direction due to the higher inertia related to this direction. Even if the buildings have a squared floor plan, these differences still exist because the inertia relative to the centered axis paralell to +X direction still continues being greater than in the +Y direction.

As a general remark and for both scenarios, the buildings analyzed as isolated show a higher vulnerability in the +X direction (short direction). Nevertheless, this conclusion is true for buildings which have a rectangular floor plan (M01 and M02), while the buildings with a more squared floor plan (M03) show closer values of fragility and, thus, damage in both directions (see Table 9 and Table 10). In addition, the aggregate buildings in this case improve the performance of the isolated buildings in the +X direction. Thus, the aggregate has a better performance as a group than the one of each isolated building composing it. These statements should be confirmed via stochastic studies on a higher number of isolated buildings and aggregates, in order to determine the trend and its validity.

A risk assessment on URM buildings of Barcelona was performed in Pujades et al., (2012) were the buildings and their models were slightly different from those analyzed in this article. The main model difference is the five stories height of those buildings, while seven stories buildings

Downloaded by [University of Genova], [serena cattari] at 23:58 02 April 2013

ACCEPTED MANUSCRIPT

ACCEPTED MANUSCRIPT

are studied herein. It is significant that in both analyses, despite the results differences showing lower values for the damage indices in this work, the same trends are observed. A better performance is obtained for the deterministic scenario than for the probabilistic one and, in both works, the buildings show lower values of the damage indices in direction +Y than in the direction +X. A careful comparison revealed differences in the buildings characteristics and in the calculation of the performance point. We analyzed herein seven stories buildings with detailed and complete models while there, more simplified buildings models of five stories were studied. In addition, Pujades et al (2012) uses the linear equivalent approach to obtain the performance point. It is well known that the linear equivalent approach leads to conservative results. For the present study the iterative approach, known as the procedure A, described in the chapter 8 (PA-8) of the ATC-40 (1996) has been preferred as being more realistic. Therefore, in our opinion, the already indicated differences in the geometry of the buildings, but mainly in the use of more realistic strength parameters and in the approach used to obtain the performance point, may explain the differences in the values of the damage indices. Nevertheless, it is also remarkable that, despite these significant differences, the same trends and comparable results are obtained in both studies, showing the robustness of the approaches and methods used.

Downloaded by [University of Genova], [serena cattari] at 23:58 02 April 2013

## 8. Conclusions

The modernist buildings of the Eixample district are emblematic constructions of Barcelona that must be preserved in spite of their overall vulnerability. In this article, an exhaustive investigation to identify all the structural characteristics of these modernist buildings has been

ACCEPTED MANUSCRIPT

ACCEPTED MANUSCRIPT

carried out. A complete knowledge of the buildings is necessary to approach any calculation involving nonlinear approaches.

We used an advanced structural model and an outstanding and internationally recognized program code to carry out the incremental nonlinear calculations of the studied URM buildings. One of the main objectives of this work has been the assessment of their seismic performance and expected damage starting from their capacity and fragility curves and calculating their damage indices which allow assessing their seismic vulnerability and risk.

The obtained results evidence that for the probabilistic scenario the buildings show higher damage values and worse performance than for the deterministic scenario; this trend is maintained for both analyzed directions.

The obtained damage indices are higher for the isolated building than for the aggregate, indicating this fact that the seismic performance is specifically improved for the analyzed aggregate. The same trend is obtained when the damage indices are calculated for deterministic and probabilistic scenarios and for both analyzed directions.

As a general remark and for both earthquake hazard scenarios, the buildings analyzed as isolated show a higher vulnerability in the +X direction (the shorter one), which is the direction in which they have a wall density slightly higher than in the +Y direction. In our opinion, rather than considering the wall density as a criterium of comparison, the mechanical parameters related to the inertia of the walls in each direction should be correlated to the damage indices in order to explain the greater vulnerability in the +X direction.

Downloaded by [University of Genova], [serena cattari] at 23:58 02 April 2013

ACCEPTED MANUSCRIPT

ACCEPTED MANUSCRIPT

The modernist URM buildings of Barcelona are undergoing a constant process of refurbishment, renovation and conventional repair. The results obtained in this study indicate that the expected seismic damage of these buildings is predominantly moderate with non-negligible values of exceedance probability related to the severe damage state. In consequence, and due to their significant seismic vulnerability, the renovation and refurbishment works should be performed considering also seismic criteria. This statement is made even if Barcelona is located in a zone of low to moderate seismicity; however, this study, as well as previous works, shows that these structures can be significantly affected by low to moderate earthquakes due to their important vulnerability.

Downloaded by [University of Genova], [serena cattari] at 23:58 02 April 2013

**Acknowledgements**

This work has been partially funded by the Spanish Government, by the European Commission and with FEDER funds, through the research projects: CGL2008-00869/BTE, CGL2011-23621, SEDUREC-CONSOLIDER-CSD2006-00060, INTERREG: POCTEFA 2007-2013/73/08, MOVE-FT7-ENV-2007-1-211590 and DESURBS-FP7-2011-261652. The authors also would like to thank Professor Francisco Rosselló for his useful bibliographical support and for his priceless observations and comments about several architectural and structural details of the URM buildings of the Eixample.

ACCEPTED MANUSCRIPT

ACCEPTED MANUSCRIPT

**References**

Ambrasseys, N. N., Simpson, K. A. & Bommer, J. J., 1996. Prediction of horizontal response spectra in Europe. Earthquake Engineering and Structural Dynamics, Volume 25, pp. 371-400.

ATC-40, 1996. *Seismic Evaluation and Retrofit of Concrete Buildings*, Redwood City, CA: Seismic Safety Commission, USA.

Barbat, A. H., Mena, U. & Yépez, F., 1998. Evaluación Probabilista del Riesgo Sísmico en Zonas Urbanas. Revista Internacional de Métodos Numéricos para Cálculo y Diseño en Ingeniería, Volume 14, pp. 247-268. [In Spanish].

Barbat, A. H., Pujades, L. G. & Lantada, N., 2006a. Performance of Buildings Under Earthquake in Barcelona, Spain. Computer-Aided Civil and Infrastructure Engineering, Volume 21, pp. 573-593.

Barbat, A. H., Lagomarsino, S. & Pujades, L. G., 2006b. Vulnerability Assessment of Dwelling Buildings.. In: C. S. Oliveira, A. Roca & X. Goula, eds. Assessing and Managing Earthquake Risk. Dordrecht, the Netherlands: Springer, pp. 115-134.

Barbat, A. H., Pujades, L. G. & Lantada, N., 2008. Seismic Damage Evaluation in Urban Areas Using the Capacity Spectrum Method: Application to Barcelona. Soil Dynamics and Earthquake Engineering, Volume 28, pp. 851-865.

Calderini C, Cattari S and Lagomarsino S. (2009). In-plane strength of unreinforced masonry piers. Earthquake Engineering and Structural Dynamics, 38(2), 243-267.

Downloaded by [University of Genova], [serena cattari] at 23:58 02 April 2013

ACCEPTED MANUSCRIPT

ACCEPTED MANUSCRIPT

Carreño, M. L., Cardona, O. D. & Barbat, A. H., 2007. Urban Seismic Risk Evaluation: A Holistic Approach. Natural Hazards, Volume 40, pp. 137-172.

CCCB, 2009. Cerdà and the Barcelona of the Future. Reality versus Project. [Online]

Available at: http://www.cccb.org/exposicio-cerda [Last access May 2012].

Cid, J., 1998. Zonación Sísmica de la ciudad de Barcelona basada en métodos de simulación numérica de efectos locales, Barcelona, Spain: Universitat Politècnica de Catalunya.

Egozcue, J. et al., 1991. A method to estimate occurrence probabilities in low seismic activity regions. Earthquake Engineering and Structural Dynamics, 20(1), pp. 43-60.

EUROSTAT, 2011. *EUROSTAT Yearbook 2010: General and Regional Statistics*. Statistical Office of the European Union, Luxembourg.

Faccioli, E. & Cauzzi, C., 2006. Macroseismic intensities for seismic scenarios estimated from instrumentally based correlations. Genève, Switzerland.

FEMA/NIBS: Federal Emergency Management Agency and National Institute of Building Sciences, 1999. *HAZUS'99 Technical Manual. Earthquake Loss Estimation Methodology*, Washington D.C. USA.

Galasco, A., Lagomarsino, S. and Penna, A. (2006). On the use of pushover analysis for existing masonry buildings. Proc. 1st. European Conference on Earthquake Engineering and Seismology, Geneva, Switzerland.

Downloaded by [University of Genova], [serena cattari] at 23:58 02 April 2013

ACCEPTED MANUSCRIPT

ACCEPTED MANUSCRIPT

Gambarotta, L. & Lagomarsino, S., 1997. Damage model for the seismic response of brick masonry shear walls. Part II: the continuum model and its aplications. Earthquake Engineering and Structural Dynamics, Issue 26, pp. 441-462.

Gonzáles, H. F., 2010. Comportamiento sísmico de edificios con muros delgados de hormigón. Aplicación a zonas de alta sismicidad de Perú. Ph. D. Thesis. Universidad Politécnica de Cataluña, Barcelona, Spain. [In Spanish].

Grünthal, G. et al., 1999. Compilation of the GSHAP Regional Seismic Hazard for Europe, Africa and the Middle East. Annali Geofis., Volume 42, pp. 1215-1223.

Irizarry, J., 2004. An Advanced Approach to Seismic Risk Assessment. Application to the Cultural Heritage and the Urban System of Barcelona. Ph. D. Thesis. Universidad Politécnica de Cataluña, Barcelona, Spain.

Jiménez, M. J., Giardini, D., Grünthal, G. A. & SESAME-Working Group, 2001. Unified Seismic Hazard Modelling throughout the Mediterranean Region. Bolletino di Geofisica Teorica ed Applicata, 42(1-2), pp. 3-18.

Kappos, A. J., 1997. Seismic damage indices for RC buildings: evaluation of concepts and procedures. Progress in Structural Engineering and Materials, 1(1), pp. 78-87.

Keneddy, R. P. et al., 1980. Probabilistic Seismic Safety Study of an Existing Nuclear Power Plant. Nuclear Engineering and Design, 59(2), pp. 315-338.

Lagomarsino, S., Galasco, A. & Penna, A., 2002. Pushover and dynamic analysis of URM buildings by means of a non-linear macro-element model. Bucharest, s.n.

Downloaded by [University of Genova], [serena cattari] at 23:58 02 April 2013

ACCEPTED MANUSCRIPT

ACCEPTED MANUSCRIPT

Lagomarsino, S., Galasco, A., Penna, A. & Cattari, S., 2008. TREMURI: Seismic Analysis Program for 3D Masonry Buildings (User Guide). Technnical Report ed. Genoa, Italy: s.n.

Lantada, N., 2007. Evaluación del Riesgo Sísmico Mediante Métodos Avanzados y Técnicas GIS. Aplicación a Barcelona. Ph. D. Thesis. Universidad Politécnica de Cataluña, Barcelona, Spain. [In Spanish].

Lantada, N., Pujades, L. & Barbat, A., 2009. Vulnerability index and capacity spectrum based methods for urban seismic risk evaluation. A comparison. Natural Hazards, Volume 51, pp. 501-524.

Milutinovic, Z. V. & Trendafiloski, G. S., 2003. WP4: Vulnerability of Current Buildings. In: RISK-UE Project Handbook. s.l.:s.n., p. 111.

Ministerio de Fomento, 1988. *NBE-AE/88 Norma Básica de la Edificación. Acciones en la Edificación*, Madrid: Spanish Official Bulletin. [In Spanish].

Ministerio de la Vivienda, 1963. *Norma MV 101-1962. Acciones en la Edificación*, Madrid: Spanish Official Bulletin. [In Spanish].

Ministerio de la Vivienda, 2006. *Código Técnico de la Edificación*, Madrid: Spanish Official Bulletin. [In Spanish].

P.I.E.T. 70, 1971. *Obras de Fábrica. Prescripciones del Instituto Eduardo Torroja*. In: Madrid, Spain: Consejo Superior de Investigaciones Científicas. [In Spanish].

Paricio, A., 2008. *Secrets d'un sistema constructiu L'Eixample.* Barcelona, Spain: Edicions UPC. [In catalan].

Downloaded by [University of Genova], [serena cattari] at 23:58 02 April 2013

ACCEPTED MANUSCRIPT

ACCEPTED MANUSCRIPT

Pujades, L. G. et al., 2012. Seismic performance of a block of buildings representative of the typical construction in the Eixample district in Barcelona (Spain). Bulletin of Earthquake Engineering, 10(1), pp. 331-349.

Schindler, R. & Bassegoda, B., 1955. *Tratado Moderno de Construcción de Edificios*. Barcelona: José Montesó Editor. [In Spanish].

Secanell, R. et al., 2004. Seismic hazard zonation of Catalonia, Spain, integrating uncertainties. Journal of Seismology, Volume 8, pp. 24-40.

US Bureau-of-the-Census, 1991. *Report WP/91, World Population Profile: 1991*, Washington: Government Printing Office. USA.

Yépez, F., Barbat, A. H. & Canas, J. A., 1996. Simulación de Escenarios del Daño Sísmico en Zonas Urbanas. Revista Internacional de Métodos Numéricos para Cálculo y Diseño en Ingeniería, Volume 12, pp. 331-358. [In Spanish].

Downloaded by [University of Genova], [serena cattari] at 23:58 02 April 2013

ACCEPTED MANUSCRIPT

ACCEPTED MANUSCRIPT

Table captions (as a list)

Table 1. Geometric properties and load conditions of the isolated building M01.

Table 2. Geometric properties and load conditions of the aggregate A01.

Table 3. Geometric properties and load conditions of the isolated building M02.

Table 4. Geometric properties and load conditions of the isolated building M03.

Table 5. Design strength of brickwork masonry for solid clay bricks (P.I.E.T. 70, 1971).

Table 6. Modal analysis results for each model.

Table 7. Binomial probability distribution of the different damage states.

Table 8. Mean values and standard deviation of the fragility curves of the analyzed buildings and aggregate for the +X and +Y directions.

Table 9. Damage states probabilities, performance point (PP) and damage index (DI) associated to the deterministic scenario. Damage states: no damage (NO), slight (SL), moderate (MO), severe (SE) and complete (CO).

Table 10. Damage states probabilities, performance point (PP) and damage index (DI) associated to the probabilistic scenario. Damage states: no damage (NO), slight (SL), moderate (MO), severe (SE) and complete (CO).

Table 11. Elastic Stiffness of the analyzed buildings.

Downloaded by [University of Genova], [serena cattari] at 23:58 02 April 2013

ACCEPTED MANUSCRIPT

ACCEPTED MANUSCRIPT

Figure captions (as a list)

Figure 1. Example of URM buildings with high seismic vulnerability. The addition of top levels to the original buildings increases even more their seismic vulnerability.

Figure 2. A view of a section of the Eixample district (CCCB, 2009).

Figure 3. Floor plan of a characteristic row of aggregate buildings located in a main street of the Eixample district of Barcelona.

Figure 4. Façades of the analyzed buildings located in Barcelona.

Figure 5. Metallic girders and iron columns at the base floor of the M01 building.

Figure 6. Cross sections of the isometric view of an isolated building (M01 in Figure 3). a) Half building. b) Base floor. c) Characteristic floor.

Figure 7. Iron beams (sliced) simply supported on the wall.

Figure 8. Architectural floor plans (building M01). a) Façade. b) Base floor. c) Side elevation. d) Intermediate floor [the dimensions are in m].

Figure 9. Floor system. Iron beams and brick vaults

Figure 10. Details of a floor system observed during the demolition of an Eixample building.

Figure 11. Example of distribution of the arches above openings.

Figure 12. Support length for the beams located above openings.

Figure 13. 5% damped elastic response spectra for the deterministic and probabilistic earthquake scenarios of Barcelona.

Figure 14. Capacity curves and capacity spectra in +X and +Y directions for the aggregate A01.

Figure 15. Capacity spectrum of building M01 and aggregate A01. Deterministic and probabilistic scenarios and direction +X.

Figure 16. Capacity spectrum of building M01 and aggregate A01. Deterministic and probabilistic scenarios and direction +Y.

Figure 17. Fragility curves in +X and +Y directions for the aggregate A01. Spectral displacements corresponding to the performance points (deterministic and probabilistic earthquake scenarios).

Figure 18. Probabilities of occurrence of each damage state. Values of Tables 9 and 10.

ACCEPTED MANUSCRIPT



Downloaded by [University of Genova], [serena cattari] at 23:58 02 April 2013

ACCEPTED MANUSCRIPT

Figure captions

Figure 1. Example of URM buildings with high seismic vulnerability. The addition of top levels to the original buildings increases even more their seismic vulnerability.

Downloaded by [University of Genova], [serena cattari] at 23:58 02 April 2013

ACCEPTED MANUSCRIPT

ACCEPTED MANUSCRIPT

Figure 2. A view of a section of the Eixample district (CCCB, 2009).

Downloaded by [University of Genova], [serena cattari] at 23:58 02 April 2013

ACCEPTED MANUSCRIPT

ACCEPTED MANUSCRIPT

Figure 3. Floor plan of a characteristic row of aggregate buildings located in a main street of the Eixample district of Barcelona.

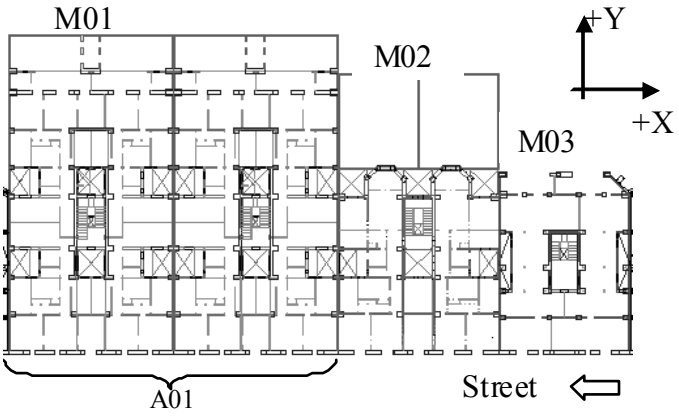


Downloaded by [University of Genova], [serena cattari] at 23:58 02 April 2013

ACCEPTED MANUSCRIPT

ACCEPTED MANUSCRIPT

Figure 4. Façades of the analyzed buildings located in Barcelona.

Downloaded by [University of Genova], [serena cattari] at 23:58 02 April 2013

ACCEPTED MANUSCRIPT

ACCEPTED MANUSCRIPT

Figure 5. Metallic girders and iron columns at the base floor of the M01 building.

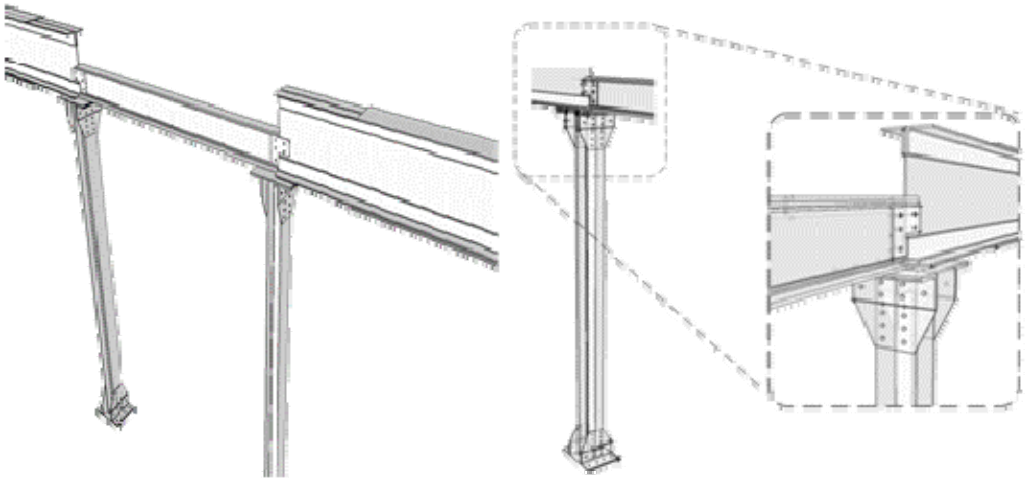

Downloaded by [University of Genova], [serena cattari] at 23:58 02 April 2013

ACCEPTED MANUSCRIPT

ACCEPTED MANUSCRIPT

Figure 6. Cross sections of the isometric view of an isolated building (M01 in Figure 3). a) Half building. b) Base floor. c) Characteristic floor.

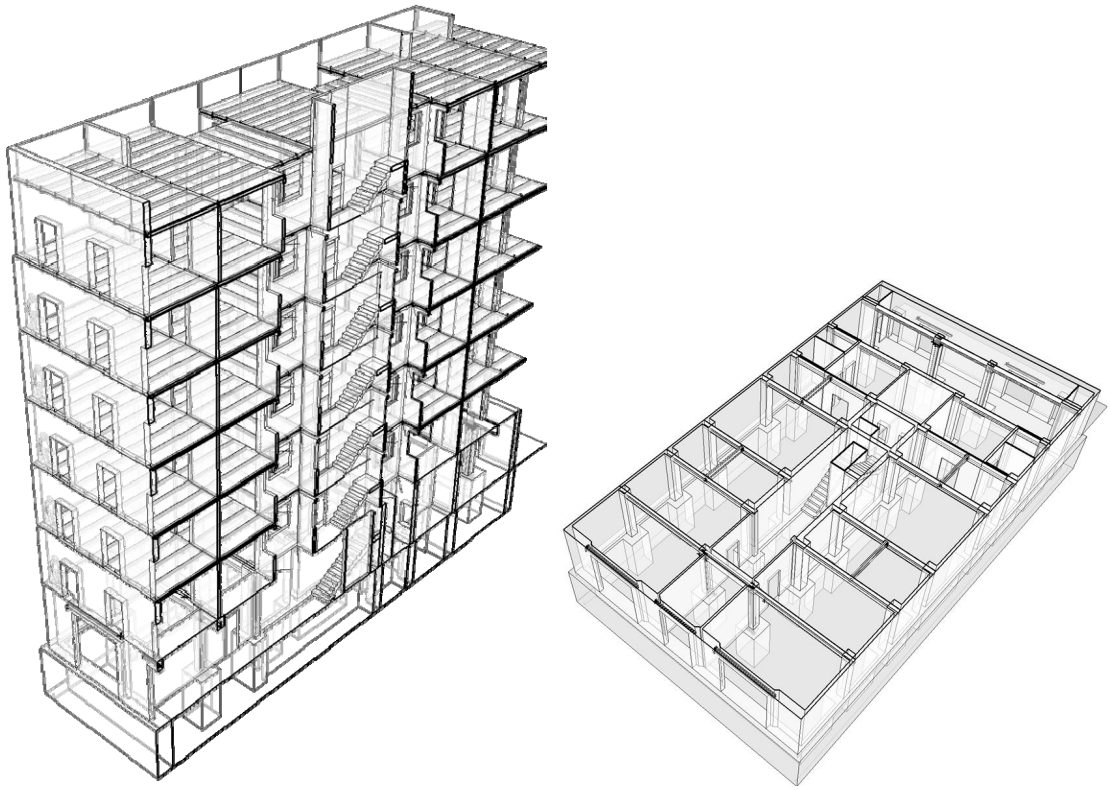

a) b)

Downloaded by [University of Genova], [serena cattari] at 23:58 02 April 2013

ACCEPTED MANUSCRIPT

ACCEPTED MANUSCRIPT

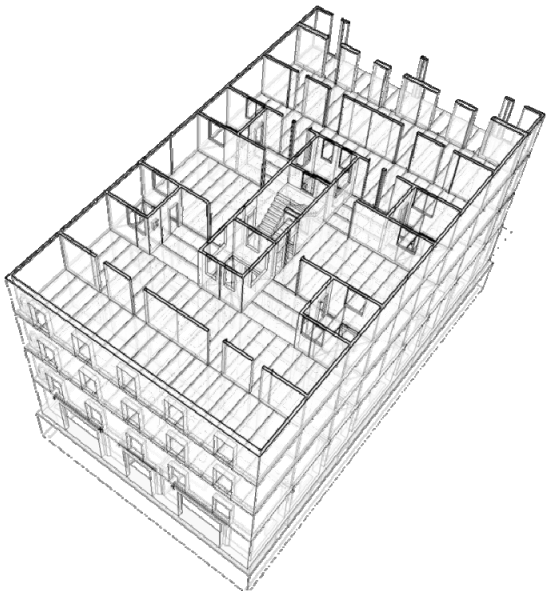

c)

Downloaded by [University of Genova], [serena cattari] at 23:58 02 April 2013

ACCEPTED MANUSCRIPT

ACCEPTED MANUSCRIPT

Figure 7. Iron beams (sliced) simply supported on the wall.

Downloaded by [University of Genova], [serena cattari] at 23:58 02 April 2013

ACCEPTED MANUSCRIPT

ACCEPTED MANUSCRIPT

Figure 8. Architectural floor plans (building M01). a) Façade. b) Base floor. c) Side elevation. d) Intermediate floor [the dimensions are in m].

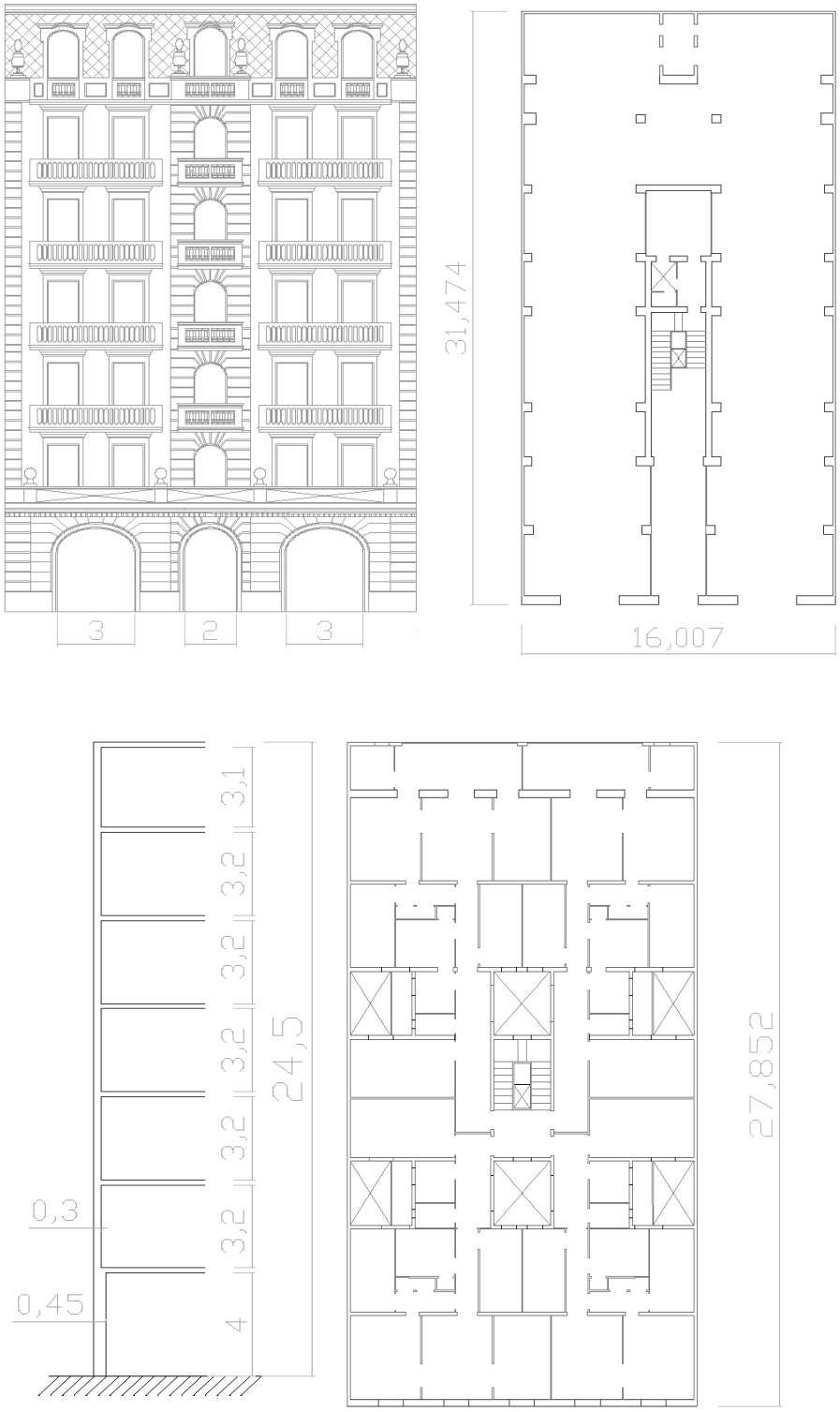


ACCEPTED MANUSCRIPT



Downloaded by [University of Genova], [serena cattari] at 23:58 02 April 2013

ACCEPTED MANUSCRIPT

Figure 9. Floor system. Iron beams and brick vaults

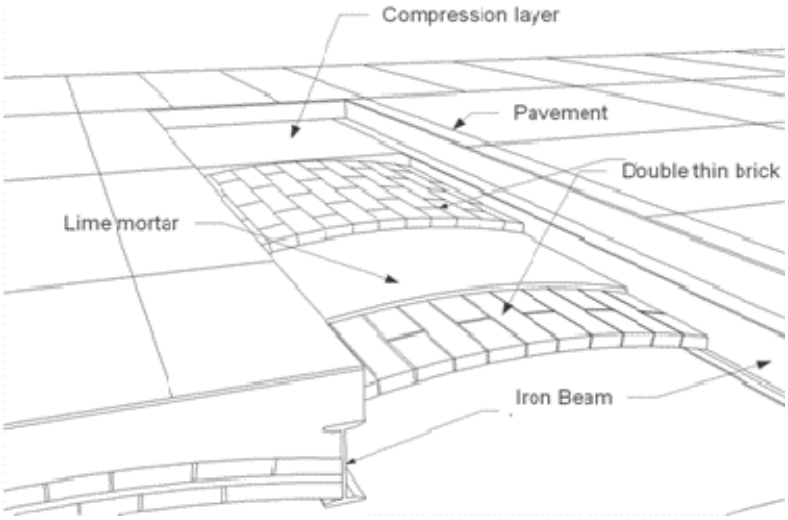


Downloaded by [University of Genova], [serena cattari] at 23:58 02 April 2013

ACCEPTED MANUSCRIPT

ACCEPTED MANUSCRIPT

Figure 10. Details of a floor system observed during the demolition of an Eixample building.

Downloaded by [University of Genova], [serena cattari] at 23:58 02 April 2013

ACCEPTED MANUSCRIPT

ACCEPTED MANUSCRIPT

Figure 11. Example of distribution of the arches above openings.

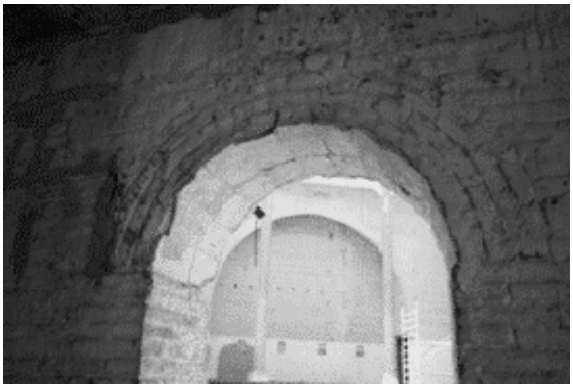

Downloaded by [University of Genova], [serena cattari] at 23:58 02 April 2013

ACCEPTED MANUSCRIPT

ACCEPTED MANUSCRIPT

Figure 12. Support length for the beams located above openings.

Downloaded by [University of Genova], [serena cattari] at 23:58 02 April 2013

ACCEPTED MANUSCRIPT

ACCEPTED MANUSCRIPT

Figure 13. 5% damped elastic response spectra for the deterministic and probabilistic earthquake scenarios of Barcelona.

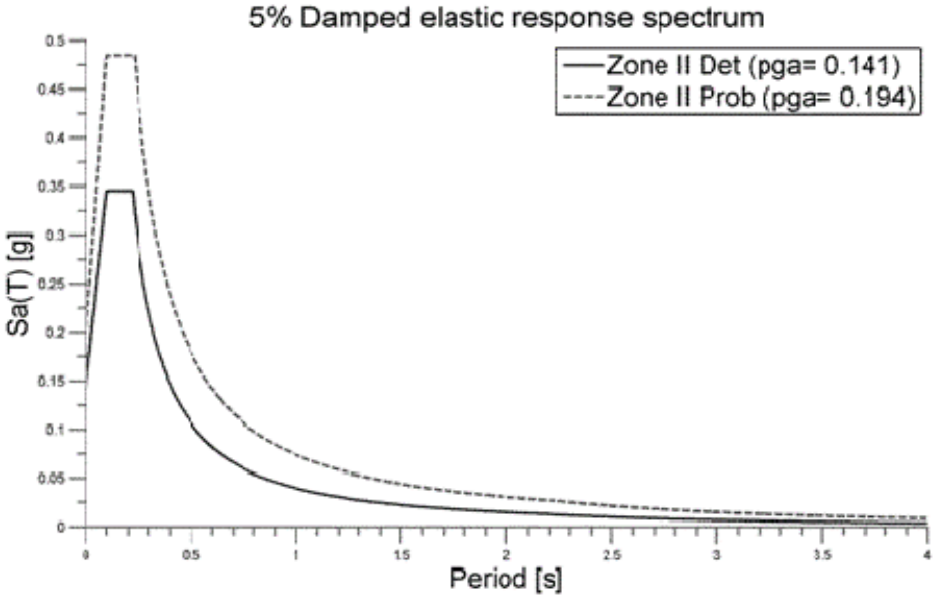


Downloaded by [University of Genova], [serena cattari] at 23:58 02 April 2013

ACCEPTED MANUSCRIPT

ACCEPTED MANUSCRIPT

Figure 14. Capacity curves and capacity spectra in +X and +Y directions for the aggregate A01.

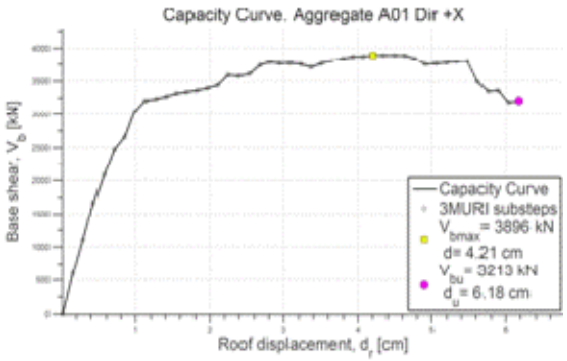


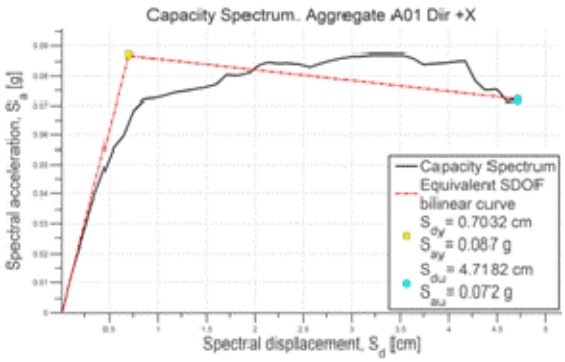


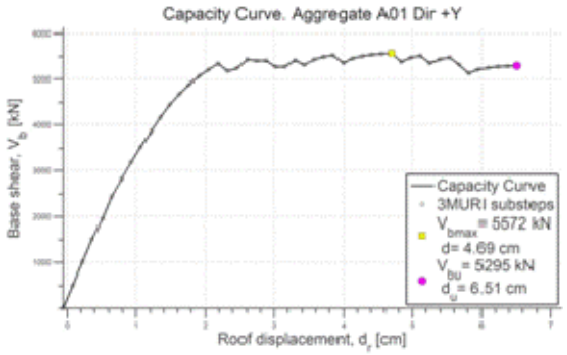


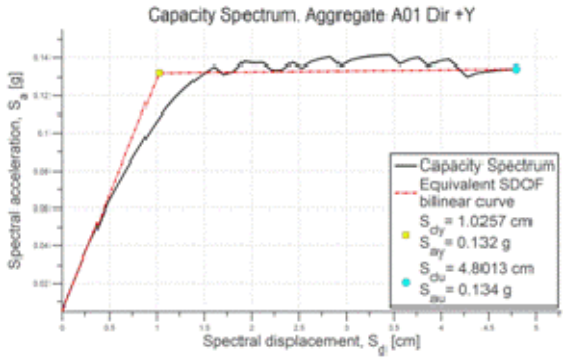


Downloaded by [University of Genova], [serena cattari] at 23:58 02 April 2013

ACCEPTED MANUSCRIPT

ACCEPTED MANUSCRIPT

Figure 15. Capacity spectrum of building M01 and aggregate A01. Deterministic and probabilistic scenarios and direction +X.

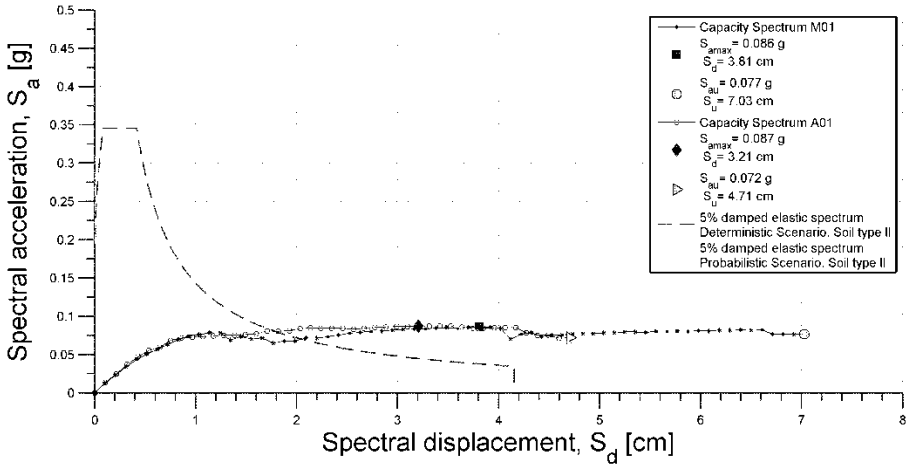


Downloaded by [University of Genova], [serena cattari] at 23:58 02 April 2013

ACCEPTED MANUSCRIPT

ACCEPTED MANUSCRIPT

Figure 16. Capacity spectrum of building M01 and aggregate A01. Deterministic and probabilistic scenarios and direction +Y.

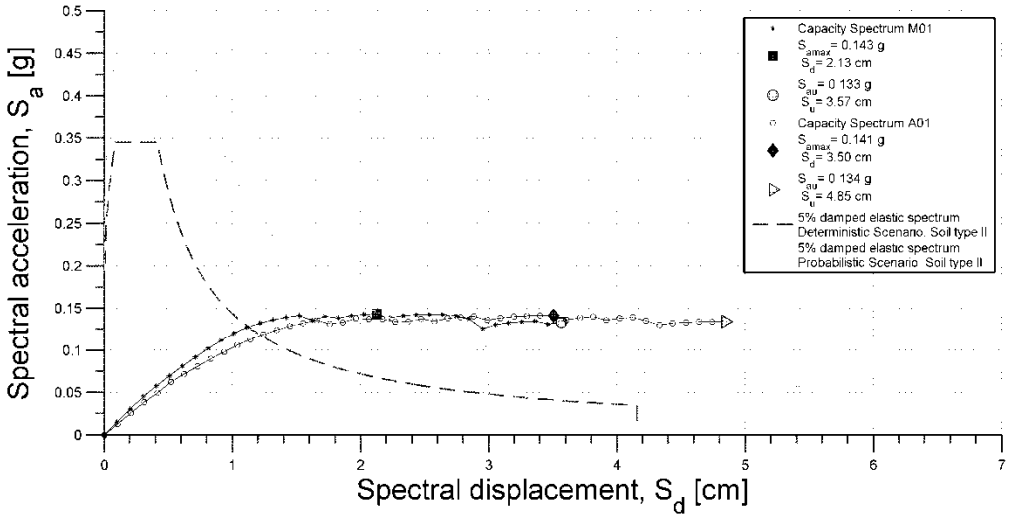


Downloaded by [University of Genova], [serena cattari] at 23:58 02 April 2013

ACCEPTED MANUSCRIPT

ACCEPTED MANUSCRIPT

Figure 17. Fragility curves in +X and +Y directions for the aggregate A01. Spectral displacements corresponding to the performance points (deterministic and probabilistic earthquake scenarios).

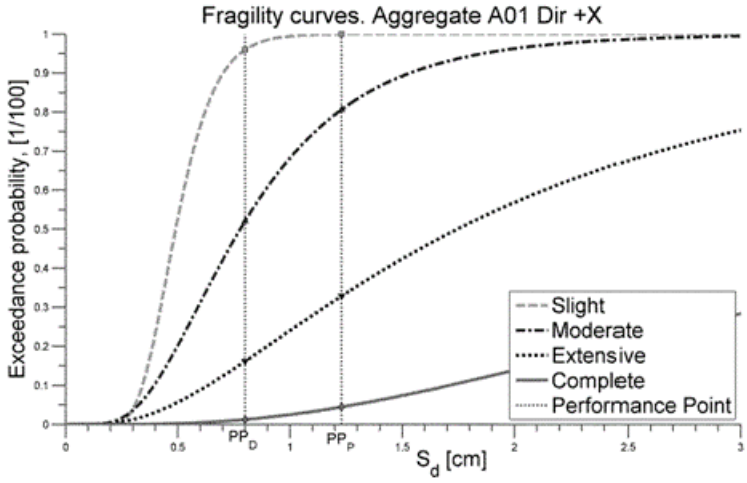


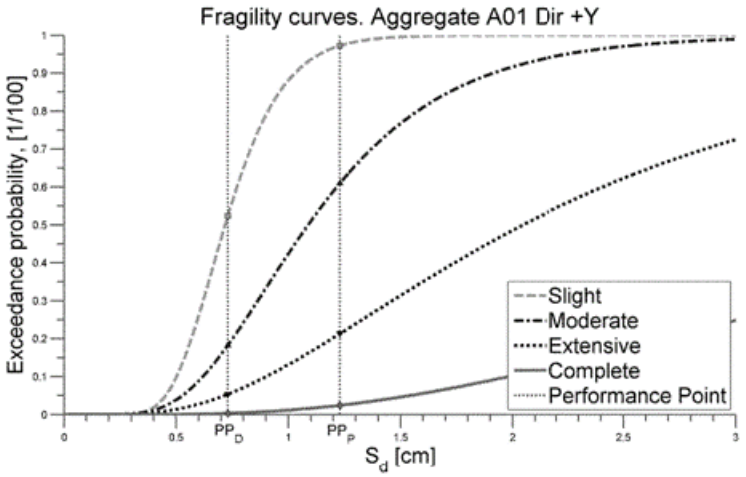


Downloaded by [University of Genova], [serena cattari] at 23:58 02 April 2013

ACCEPTED MANUSCRIPT

ACCEPTED MANUSCRIPT

Figure 18. Probabilities of occurrence of each damage state. Values of Tables 9 and 10.

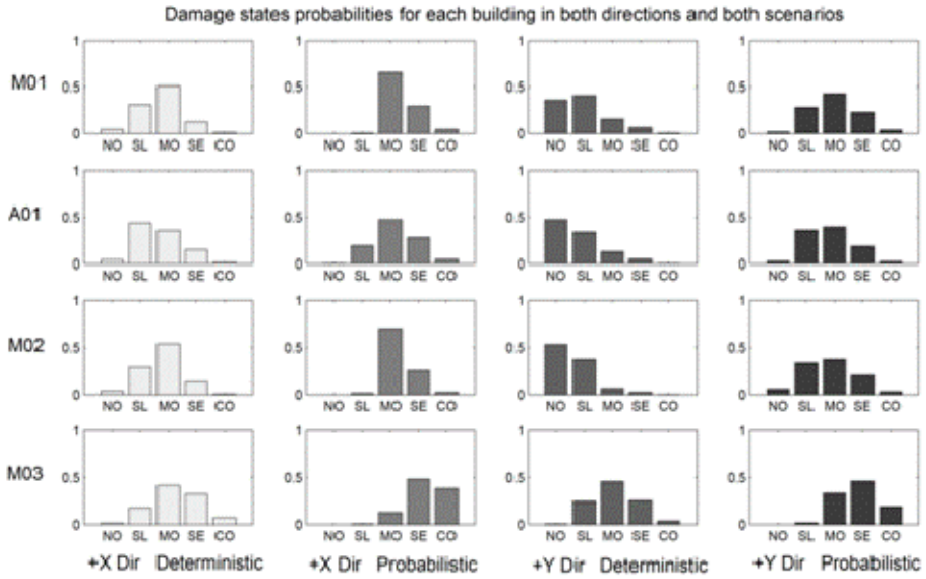


Downloaded by [University of Genova], [serena cattari] at 23:58 02 April 2013

ACCEPTED MANUSCRIPT

ACCEPTED MANUSCRIPT

**Table captions**

Table 1. Geometric properties and load conditions of the isolated building M01.

| | | | Story | | | | | | |
|---|---|---|---|---|---|---|---|---|---|
| | | | **1** | **2** | **3** | **4** | **5** | **6** | **7** |
| | **Story Height (cm)** | | 420 | 340 | 340 | 340 | 340 | 340 | 330 |
| | **Walls density** | | 0,089 | 0,059 | 0,059 | 0,059 | 0,059 | 0,059 | 0,059 |
| | **Walls density** | **+X Dir** | 0,029 | 0,037 | 0,037 | 0,037 | 0,037 | 0,037 | 0,037 |
| | | **+Y Dir** | 0,059 | 0,022 | 0,022 | 0,022 | 0,022 | 0,022 | 0,022 |
| | **Dead load (daN)** | | 350 | 350 | 350 | 350 | 350 | 350 | 350 |
| | **Live load (daN)** | | 200 | 200 | 200 | 200 | 200 | 200 | 100 |
| **Walls Thickness** | **Main façade** | | 45 | 30 | 30 | 30 | 30 | 30 | 30 |
| | **Post facade** | | 30 | 30 | 30 | 30 | 30 | 30 | 30 |

Downloaded by [University of Genova], [serena cattari] at 23:58 02 April 2013

ACCEPTED MANUSCRIPT

ACCEPTED MANUSCRIPT

| | | | | | | | | |
|---|---|---|---|---|---|---|---|---|
| **(cm)** | **Staircases** | 30 | 15 | 15 | 15 | 15 | 15 | 15 |
| | **Inner bearing walls** | | 15 | 15 | 15 | 15 | 15 | 15 |
| | **Intermediate bearing walls** | 30 | 15 | 15 | 15 | 15 | 15 | 15 |
| | **Distribution walls** | | 5 | 5 | 5 | 5 | 5 | 5 |

Downloaded by [University of Genova], [serena cattari] at 23:58 02 April 2013

ACCEPTED MANUSCRIPT

ACCEPTED MANUSCRIPT

Table 2. Geometric properties and load conditions of the aggregate A01.

| | | | Story | | | | | | |
|---|---|---|---|---|---|---|---|---|---|
| | | | **1** | **2** | **3** | **4** | **5** | **6** | **7** |
| | **Story Height (cm)** | | 420 | 340 | 340 | 340 | 340 | 340 | 330 |
| | **Walls density** | | 0,089 | 0,059 | 0,059 | 0,059 | 0,059 | 0,059 | 0,059 |
| | **Walls density** | **+X Dir** | 0,029 | 0,037 | 0,037 | 0,037 | 0,037 | 0,037 | 0,037 |
| | | **+Y Dir** | 0,041 | 0,022 | 0,022 | 0,022 | 0,022 | 0,022 | 0,022 |
| | **Dead load (daN)** | | 350 | 350 | 350 | 350 | 350 | 350 | 350 |
| | **Live load (daN)** | | 200 | 200 | 200 | 200 | 200 | 200 | 100 |
| **Walls Thickness (cm)** | **Main façade** | | 45 | 30 | 30 | 30 | 30 | 30 | 30 |
| | **Post facade** | | 30 | 30 | 30 | 30 | 30 | 30 | 30 |
| | **Staircases** | | 30 | 15 | 15 | 15 | 15 | 15 | 15 |

ACCEPTED MANUSCRIPT



Downloaded by [University of Genova], [serena cattari] at 23:58 02 April 2013

ACCEPTED MANUSCRIPT

| | | | | | | | |
|---|---|---|---|---|---|---|---|
| **Inner bearing walls** | | 15 | 15 | 15 | 15 | 15 | 15 |
| **Intermediate bearing walls** | 30 | 30 | 30 | 30 | 30 | 30 | 30 |
| **Distribution walls** | | 5 | 5 | 5 | 5 | 5 | 5 |

Downloaded by [University of Genova], [serena cattari] at 23:58 02 April 2013

ACCEPTED MANUSCRIPT

ACCEPTED MANUSCRIPT

Table 3. Geometric properties and load conditions of the isolated building M02.

| | | | Story | | | | | | |
|---|---|---|---|---|---|---|---|---|---|
| | | | **1** | **2** | **3** | **4** | **5** | **6** | **7** |
| | **Story Height (cm)** | | 420 | 340 | 340 | 340 | 340 | 340 | 330 |
| | **Walls density** | | 0,107 | 0,062 | 0,062 | 0,062 | 0,062 | 0,062 | 0,062 |
| | **Walls density** | **+X Dir** | 0,028 | 0,034 | 0,034 | 0,034 | 0,034 | 0,034 | 0,034 |
| | | **+Y Dir** | 0,079 | 0,028 | 0,028 | 0,028 | 0,028 | 0,028 | 0,028 |
| | **Dead load (daN)** | | 350 | 350 | 350 | 350 | 350 | 350 | 350 |
| | **Live load (daN)** | | 200 | 200 | 200 | 200 | 200 | 200 | 100 |
| **Walls Thickness (cm)** | **Main façade** | | 45 | 30 | 30 | 30 | 30 | 30 | 30 |
| | **Post facade** | | 45 | 30 | 30 | 30 | 30 | 30 | 30 |
| | **Staircases** | | 30 | 15 | 15 | 15 | 15 | 15 | 15 |

ACCEPTED MANUSCRIPT



Downloaded by [University of Genova], [serena cattari] at 23:58 02 April 2013

ACCEPTED MANUSCRIPT

| | | | | | | | |
|---|---|---|---|---|---|---|---|
| **Inner bearing walls** | 15 | 15 | 15 | 15 | 15 | 15 | 15 |
| **Intermediate bearing walls** | 30 | 15 | 15 | 15 | 15 | 15 | 15 |
| **Distribution walls** | | 5 | 5 | 5 | 5 | 5 | 5 |

Downloaded by [University of Genova], [serena cattari] at 23:58 02 April 2013

ACCEPTED MANUSCRIPT

ACCEPTED MANUSCRIPT

Table 4. Geometric properties and load conditions of the isolated building M03.

| | | | Story | | | | | | |
|---|---|---|---|---|---|---|---|---|---|
| | | | **1** | **2** | **3** | **4** | **5** | **6** | **7** |
| **Story Height (cm)** | | | 420 | 340 | 340 | 340 | 340 | 340 | 330 |
| **Walls density** | | | 0,092 | 0,068 | 0,068 | 0,068 | 0,068 | 0,068 | 0,068 |
| **Walls density** | | **+X Dir** | 0,034 | 0,035 | 0,035 | 0,035 | 0,035 | 0,035 | 0,035 |
| | | **+Y Dir** | 0,058 | 0,033 | 0,033 | 0,033 | 0,033 | 0,033 | 0,033 |
| **Dead load (daN)** | | | 350 | 350 | 350 | 350 | 350 | 350 | 350 |
| **Live load (daN)** | | | 200 | 200 | 200 | 200 | 200 | 200 | 100 |
| **Walls Thickness (cm)** | **Main façade** | | 45 | 30 | 30 | 30 | 30 | 30 | 30 |
| | **Post facade** | | 45 | 30 | 30 | 30 | 30 | 30 | 30 |
| | **Staircases** | | 30 | 15 | 15 | 15 | 15 | 15 | 15 |

ACCEPTED MANUSCRIPT



Downloaded by [University of Genova], [serena cattari] at 23:58 02 April 2013

ACCEPTED MANUSCRIPT

| | | | | | | | |
|---|---|---|---|---|---|---|---|
| **Inner bearing walls** | | 15 | 15 | 15 | 15 | 15 | 15 |
| **Intermediate bearing walls** | 30 | 15 | 15 | 15 | 15 | 15 | 15 |
| **Distribution walls** | | 5 | 5 | 5 | 5 | 5 | 5 |

Downloaded by [University of Genova], [serena cattari] at 23:58 02 April 2013

ACCEPTED MANUSCRIPT

ACCEPTED MANUSCRIPT

Table 5. Design strength of brickwork masonry for solid clay bricks (P.I.E.T. 70, 1971).

| Brick strength (MPa) | Mortar plasticity | Joint thickness (cm) | Design strength of brickwork using mortar (MPa) | | | | | |
|---|---|---|---|---|---|---|---|---|
| | | | M-5 | M-10 | M-20 | M-40 | M-80 | M-160 |
| 7 | Low | >1,5 | 0,8 | 0,9 | 1,0 | 1,1 | 1,2 | - |
| | Low<br>Medium | 1 to 1,5<br>>1,5 | 0,9 | 1,0 | 1,1 | 1,2 | 1,4 | - |
| | Low<br>Medium<br>High | <1<br>1 to 1,5<br>>1,5 | 1,0 | 1,1 | 1,2 | 1,4 | 1,6 | - |
| | Medium<br>High | <1<br>1 to 1,5 | 1,1 | 1,2 | 1,4 | 1,6 | 1,8 | - |

Downloaded by [University of Genova], [serena cattari] at 23:58 02 April 2013

ACCEPTED MANUSCRIPT

ACCEPTED MANUSCRIPT

| | | | | | | | | |
|---|---|---|---|---|---|---|---|---|
| | High | <1 | 1,2 | 1,4 | 1,6 | 1,8 | 2,0 | - |
| | Low | >1,5 | | | | | | |
| | Low | 1 to 1,5 | 1,4 | 1,6 | 1,8 | 2,0 | 2,2 | 2,5 |
| | Medium | >1,5 | | | | | | |
| | Low | <1 | | | | | | |
| | Medium | 1 to 1,5 | 1,6 | 1,8 | 2,0 | 2,2 | 2,5 | 2,8 |
| 15 | High | >1,5 | | | | | | |
| | Medium | <1 | 1,8 | 2,0 | 2,2 | 2,5 | 2,8 | 3,2 |
| | High | 1 to 1,5 | | | | | | |
| | High | <1 | 2,0 | 2,2 | 2,5 | 2,8 | 3,2 | 3,6 |
| | Low | >1,5 | | | | | | |
| 30 | Low | 1 to 1,5 | 2,2 | 2,5 | 2,8 | 3,2 | 3,6 | 4,0 |

Downloaded by [University of Genova], [serena cattari] at 23:58 02 April 2013

ACCEPTED MANUSCRIPT

ACCEPTED MANUSCRIPT

| | | | | | | | |
|---|---|---|---|---|---|---|---|
| Medium | >1,5 | | | | | | |
| Low | <1 | | | | | | |
| Medium | 1 to 1,5 | 2,5 | 2,8 | 3,2 | 3,6 | 4,0 | 4,5 |
| High | >1,5 | | | | | | |
| Medium | <1 | | | | | | |
| High | 1 to 1,5 | 2,8 | 3,2 | 3,6 | 4,0 | 4,5 | 5,0 |
| High | <1 | 3,2 | 3,6 | 4,0 | 4,5 | 5,0 | 5,6 |

Downloaded by [University of Genova], [serena cattari] at 23:58 02 April 2013

ACCEPTED MANUSCRIPT

ACCEPTED MANUSCRIPT

Table 6. Modal analysis results for each model.

| | Buildings | | | | |
|---|---|---|---|---|---|
| | | M01 | A01 | M02 | M03 |
| | Mode | Period T[s] | Period T[s] | Period T[s] | Period T[s] |
| Translation | 1 | 0,54770 | 0,57124 | 0,68759 | 0,66808 |
| Translation | 2 | 0,53658 | 0,54403 | 0,56238 | 0,52099 |
| Rotation | 3 | 0,46824 | 0,50208 | 0,52485 | 0,49452 |

Downloaded by [University of Genova], [serena cattari] at 23:58 02 April 2013

ACCEPTED MANUSCRIPT

ACCEPTED MANUSCRIPT

Table 7. Binomial probability distribution of the different damage states.

| | $P(ds_1)$ | $P(ds_2)$ | $P(ds_3)$ | $P(ds_4)$ |
|---|---|---|---|---|
| $P(ds_1)=0,5$ | **0,50** | 0,119 | 0,012 | 0,00 |
| $P(ds_2)=0,5$ | 0,896 | **0,50** | 0,135 | 0,008 |
| $P(ds_3)=0,5$ | 0,992 | 0,866 | **0,50** | 0,104 |
| $P(ds_4)=0,5$ | 1 | 0,988 | 0,881 | **0,50** |

Downloaded by [University of Genova], [serena cattari] at 23:58 02 April 2013

ACCEPTED MANUSCRIPT

ACCEPTED MANUSCRIPT

Table 8. Mean values and standard deviation of the fragility curves of the analyzed buildings and aggregate for the +X and +Y directions.

| Building | Direction | $Sd_1$ [cm] | $\beta_1$ | $Sd_2$ [cm] | $\beta_2$ | $Sd_3$ [cm] | $\beta_3$ | $Sd_4$ [cm] | $\beta_4$ |
|---|---|---|---|---|---|---|---|---|---|
| M01 | X | 0,49 | 0,28 | 0,70 | 0,31 | 2,27 | 0,95 | 7,02 | 0,88 |
| | Y | 0,64 | 0,28 | 0,94 | 0,39 | 1,63 | 0,57 | 3,55 | 0,63 |
| A01 | X | 0,49 | 0,28 | 0,78 | 0,53 | 1,74 | 0,79 | 4,71 | 0,79 |
| | Y | 0,72 | 0,28 | 1,09 | 0,44 | 2,05 | 0,64 | 4,80 | 0,69 |
| M02 | X | 0,53 | 0,28 | 0,76 | 0,30 | 2,54 | 0,97 | 7,97 | 0,89 |
| | Y | 0,74 | 0,28 | 1,05 | 0,29 | 1,50 | 0,38 | 2,60 | 0,45 |
| M03 | X | 0,48 | 0,28 | 0,68 | 0,30 | 0,98 | 0,39 | 1,72 | 0,46 |
| | Y | 0,41 | 0,28 | 0,62 | 0,43 | 1,18 | 0,64 | 2,75 | 0,69 |

Downloaded by [University of Genova], [serena cattari] at 23:58 02 April 2013

ACCEPTED MANUSCRIPT

ACCEPTED MANUSCRIPT

Table 9. Damage states probabilities, performance point (PP) and damage index (DI) associated to the deterministic scenario. Damage states: no damage (NO), slight (SL), moderate (MO), severe (SE) and complete (CO).

| | | Deterministic | | | | | | |
|---|---|---|---|---|---|---|---|---|
| | Dir | NO [%] | SL [%] | MO [%] | SE [%] | CO [%] | PP [cm] | D I [%] |
| M01 | +X | 4,3 | 31,2 | 51,1 | 12,7 | 0,7 | 0,79 | 43,5 |
| | +Y | 36,4 | 40,9 | 15,8 | 6,4 | 0,5 | 0,70 | 23.4 |
| A01 | +X | 4,1 | 43,9 | 35,9 | 14,9 | 1,2 | 0,80 | 41,4 |
| | +Y | 47,7 | 34,1 | 12,9 | 5,0 | 0,3 | 0,73 | 19.1 |
| M02 | +X | 3,8 | 28,7 | 54,1 | 12,8 | 0,6 | 0,87 | 44,4 |
| | +Y | 53,3 | 37,3 | 6,8 | 2,4 | 0,2 | 0,72 | 14,7 |
| M03 | +X | 1,4 | 18,0 | 41,3 | 32,0 | 7,3 | 0,88 | 56,4 |
| | +Y | 0,6 | 24,5 | 45,7 | 25,1 | 4,1 | 0,83 | 51,9 |

Downloaded by [University of Genova], [serena cattari] at 23:58 02 April 2013

ACCEPTED MANUSCRIPT

ACCEPTED MANUSCRIPT

Downloaded by [University of Genova], [serena cattari] at 23:58 02 April 2013

ACCEPTED MANUSCRIPT

ACCEPTED MANUSCRIPT

Table 10. Damage states probabilities, performance point (PP) and damage index (DI) associated to the probabilistic scenario. Damage states: no damage (NO), slight (SL), moderate (MO), severe (SE) and complete (CO).

| | | Probabilistic | | | | | | |
|---|---|---|---|---|---|---|---|---|
| | Dir | NO [%] | SL [%] | MO [%] | SE [%] | CO [%] | PP [cm] | D I [%] |
| M01 | +X | 0,0 | 0,6 | 65,4 | 29,8 | 4,2 | 1,53 | 59,4 |
| | +Y | 1,7 | 28,4 | 43,0 | 23,2 | 3,7 | 1,15 | 49,7 |
| A01 | +X | 0,1 | 19,3 | 47,7 | 28,4 | 4,5 | 1,23 | 54,5 |
| | +Y | 2,7 | 36,3 | 39,7 | 18,9 | 2,4 | 1,23 | 45,5 |
| M02 | +X | 0,0 | 1,6 | 70,5 | 25,2 | 2,7 | 1,44 | 57,2 |
| | +Y | 6,0 | 33,4 | 37,2 | 20,0 | 3,4 | 1,14 | 45,4 |
| M03 | +X | 0,0 | 0,4 | 13,3 | 48,0 | 38,3 | 1,50 | 81,0 |
| | +Y | 0,0 | 2,0 | 32,9 | 45,9 | 19,2 | 1,51 | 70,6 |

Downloaded by [University of Genova], [serena cattari] at 23:58 02 April 2013

ACCEPTED MANUSCRIPT

ACCEPTED MANUSCRIPT

Downloaded by [University of Genova], [serena cattari] at 23:58 02 April 2013

ACCEPTED MANUSCRIPT

ACCEPTED MANUSCRIPT

Table 11. Elastic Stiffness of the analyzed buildings.

| Building | Elastic Stiffness | |
|---|---|---|
| | +X direction $K_x$ (kN/cm) | +Y direction $K_y$ (kN/cm) |
| M01 | 1900 | 2100 |
| A01 | 4000 | 4000 |
| M02 | 900 | 1250 |
| M03 | 625 | 800 |

Downloaded by [University of Genova], [serena cattari] at 23:58 02 April 2013

ACCEPTED MANUSCRIPT